MHD Mixed Convective Flow of Maxwell Nanofluid Past a Porous Vertical Stretching Sheet in Presence of Chemical Reaction

Hunegnaw Dessie
Debre Markos University

Demeke Fissha
Debre Markos University

Recommended Citation

MHD Mixed Convective Flow of Maxwell Nanofluid Past a Porous Vertical Stretching Sheet in Presence of Chemical Reaction

[1*]**Hunegnaw Dessie and [2]Demeke Fissha**

Department of Mathematics
Debre Markos University
Debre Markos, Ethiopia
[1]tewdroshunex@gmail.com; [2]demeke19@gmail.com

*Corresponding author

Abstract

In this study, MHD mixed convective flow of Maxwell nanofluid past a porous vertical stretching sheet in the presence of chemical reaction is investigated. The governing partial differential equations with the corresponding boundary conditions are reduced to a set of ordinary differential equations via Lie group analysis. Numerical solutions of these equations are obtained by Runge-Kutta fourth order method along with shooting technique and the results obtained for different governing flow parameters are drawn graphically and their effects on velocity, temperature and concentration profiles are discussed. The values of skin-friction coefficient, Nusselt number coefficient and Sherwood number coefficient are presented in table. A comparison with previously reported data is made and an excellent agreement is noted.

1. Introduction

The topic of heat transfer via porous media has been a hot subject due to its technological and engineering applications. Examples may include packed sphere beds, electrochemical processes, grain storage, insulation for buildings and lining of nuclear reactors, regeneration of heat exchangers, chemical catalytic reactors and solar power collectors. Flagged investigations in this

530

Applications and Applied Mathematics: An International Journal (AAM), Vol. 15 [], Iss. 1, Art. 31

AAM: Intern. J., Vol. 15, Issue 1 (June 2020)   531

core area include numerous studies like Shehzad et al. (2016) who examined 3D flow of Casson fluid through porous media. They carried out analysis in the presence of heat generation/absorption. Sheikholeslami et al. (2014) debated flow of viscous nanofluid through a porous medium with four different nanomaterials and water as base fluid. Hayat et al. (2013) explored influence of convective boundary conditions on magnetohydrodynamic (MHD) nanofluid flow through a porous medium over an exponentially stretching sheet using series solution technique. Makinde et al. (2016) studied effects of unsteady magnetohydrodynamic, thermal radiation, chemical reaction and thermophoresis on a vertical porous plate. They employed sixth order RK-technique accompanied by Nachtsheim and Swigert's shooting method. It was noticed that skin friction coefficient decreases and local Nusselt number increases against gradual growing values of unsteady viscosity parameter. Extensive literature is also available pertaining flows through porous medium with most recent investigations referred at Ellahi et al. (2015), Ramesh (2016) and Ahamd et al. (2016).

Nomenclature

a, b, c	dimensional constants	Sh_x	Sherwood number
M	magnetic parameter	s	Suction parameter
C	concentration of fluid	Sr	Soret number
c_p	Specific heat	T	temperature of fluid
c_s	concentration susceptibility	T_m	mean fluid temperature
c_w	concentration on wall	T_w	wall temperature
K	Chemical reaction parameter	T_∞	Ambient temperature
c_∞	ambient concentration	(u, v)	velocity components
D_B	Brownian motion coefficient	$u_w(x)$	stretching velocity along x-axis
D_e	mass diffusivity	V_0	stretching velocity along y-axis
D_f	DuFour number	(x, y)	coordinate axis
D_T	Thermophoretic diffusion coeff.	α_m	thermal diffusivity
f'	Dimensionless velocity	β_T	coefficient of thermal expansion
g	Thermophoretic diffusion coefficient	β_c	Coefficient of concentration expansion
Gr_x	Grashof number	β	Deborah number
j_w	mass flux	γ	porosity parameter
k	thermal conductivity	ρ	density of fluid
K'	permeability constant	λ	Mixed convection parameter
Le	Lewis number	λ_1	relaxation time parameter
N	Buoyancy ratio parameter	v	Kinematic viscosity
Nb	Brownian motion parameter	ψ	Stream function
Nt	thermophoresis parameter	θ	Dimensionless temperature
Nu_x	Nusselt number	η	Similarity variable
Pr	Prandtl number	φ	Dimensionless concentration
q_w	Surface heat flux	τ	Ratio of effective heat capacity of nanoparticle and base fluid

Recent studies have given a significant attention to non-Newtonian fluid flows which are produced by stretched surfaces. The non-Newtonian flows have wide range applications in engineering including aerodynamic emission of plastic films, thinning and annealing of copper wires and liquid film condensation process etc. (Yilmazoglu et al. (2013)). Unlike viscous fluids, an obvious hurdle in mathematical modelling of these fluids is that a single constitutive equation cannot exhibit all characteristics of these fluid structures. That is why several non-Newtonian fluids models have been suggested by researchers in the literature. Maxwell fluid, which is a class

of viscoelastic fluid, can be quoted to represent the characteristics of fluid relaxation time. Here, shear-dependent viscosity's complicated effects are excluded and allow one to focus on the influence of elasticity of fluid on boundary layer characteristics. A pioneering work by Harris (1977) on 2D flow of upper convected Maxwell fluid encouraged follower researchers to investigate more avenues in this direction. Sadeghy et al. (2005) proposed local similarity solutions by four dissimilar approaches with the findings that velocity decreases with an increase in local Deborah number. They considered Maxwell fluid flow over a moving flat plate known as Sakiadis flow. Kumari et al. (2009) discussed numerical solution of mixed convection stagnation point Maxwell fluid flow using finite difference method. Hayat et al. (2009) found series solution of stagnation point magnetohydrodynamic flow over a stretching surface of an upper-convected Maxwell fluid. Motivated from above works, researchers have investigated two and three dimensional Maxwell fluid flows in numerous scenarios (see Shafique et al. (2016), Awais et al. (2015), Nadeem et al. (2014), Qayyum et al. (2014) and Abbasi et al. (2006)).

The term nanofluid is defined as a solid–liquid mixture consisting of nanoparticles and a base liquid. Choi is the first to use the term nanofluids to refer to fluids with suspended nanoparticles. Studies have shown that adding nanoparticles to a base fluid can effectively improve the thermal conductivity of the base fluid and enhance heat transfer performance of the liquid. This is why nanofluids have found such a wide range of applications in so many fields such as energy, power, aerospace, aviation, vehicles, electronics, etc. The thermal conductivity of the nanofluids is higher than that of base fluids. Further, the novel properties of Brownian motion and thermophoresis of such fluids make them potentially useful. Nanoparticles are used to enhance the thermal characteristics of ordinary base fluids such as water, ethylene glycol or oil. In addition, the magneto-nanofluid is a unique material that has both liquid and magnetic properties. Such nanofluid has superficial role in blood analysis and cancer therapy. Buongiorno (2006) provided a mathematical model of nanofluid which has the characteristics of thermophoresis and Brownian motion. Later on, Makinde et al. (2011) investigated the boundary layer flow of viscous nanofluid with convective thermal boundary condition. Ul Haq et al. (2015) examined the two dimensional boundary layer flow of natural convective micropolar nanofluid along a vertically stretching sheet. Noor et al. (2015) investigated the mixed convection boundary layer flow of a micropolar nanofluid near a stagnation point along a vertical stretching sheet. Ibrahim et al. (2015) studied boundary layer flow of magnetohydrodynamic stagnation point flow past a stretching sheet with convective heating. Ramesh et al. (214) studied the influence of heat source/sink on a Maxwell fluid over a stretching surface with convective boundary condition in the presence of nanoparticles.

The study of heat transfer with chemical reaction in the presence nanofluids is of great practical importance to engineers and scientists because of its almost universal occurrence in many branches of science and engineering. Possible applications of this type of flow can be found in many industries. In many engineering applications such as nuclear reactor safety, combustion systems, solar collectors, metallurgy and chemical engineering, there are many transport processes that are governed by the joint action of the buoyancy forces from both thermal and mass diffusion in the presence of chemical reaction effects. Radiative flows are encountered in countless industrial and environmental processes such as heating and cooling chambers, fossil fuel combustion and energy processes, evaporation from large open water reservoirs, astrophysical flows and solar power technology. However, the thermal radiation heat transfer

Applications and Applied Mathematics: An International Journal (AAM), Vol. 15 [], Iss. 1, Art. 31

AAM: Intern. J., Vol. 15, Issue 1 (June 2020)   533

effects on different flows are very important in high temperature processes and space technology. Bhattacharyya et al. (2011) studied chemically reactive solute distribution in MHD boundary layer flow over a permeable stretching sheet with suction/injection. Unsteady MHD boundary layer flow with diffusion and first order chemical over a permeable sheet with suction or blowing is studied by Bahttacharrya et al. (2011, 2013)). Hady et al. (2012) analyzed the boundary layer flow and heat transfer characteristics of a viscous nanofluid over a nonlinearly stretching sheet in the presence of thermal radiation and variable wall temperature. Eshetu et al. (2015) investigated the boundary layer flow of nanofluids over a moving surface in the presence of thermal radiation, viscous dissipation and chemical reaction. Heat and mass transfer in MHD micropolar fluid in the presence of Diffusion thermo and chemical reaction is analyzed by KiranKumar et al. (2016).

The principal aim of the present work is to study the MHD mixed convective flow of Maxwell nanofluid past a porous vertically stretching sheet in the presence of chemical reaction. Lie's scaling` group transformations (also known as Lie group analysis or as symmetry analysis) can be used to obtain similarity transformations that can reduce a system of governing partial differential equations and associated boundary conditions to a system of ordinary differential equations. With this transformation, a third order and a second order ordinary differential equations corresponding to momentum, energy and concentration equations are derived. These equations are solved with the help of Runge Kutta fourth order along with shooting technique. The effects of different flow parameters on velocity, temperature and concentration profiles are investigated and analyzed with the help of graphical representation.

2. Mathematical Formulation

Consider a steady two dimensional Maxwell nanofluid flow past a vertical stretching sheet with variable velocity $u_w(x)$, variable temperature $T_w(x)$, variable concentration $C_w(x)$, a uniform ambient temperature T_∞ and a uniform ambient concentration C_∞ in a porous medium. A uniform magnetic field B is applied in opposite to the direction of the fluid flow. Amalgamated effects of Soret and DuFour are considered. We also considered the buoyancy effects and density variation in the given flow. Bossineq approximation is taken for both energy or temperature and concentration profiles. The continuity, momentum, energy and concentration equations governing such type of flow in the presence of chemical reaction are written as below:

Continuity Equation:

$$\frac{\partial u}{\partial x} + \frac{\partial v}{\partial y} = 0. \tag{1}$$

Momentum Equation:

$$u\frac{\partial u}{\partial x} + v\frac{\partial u}{\partial y} = v\frac{\partial^2 u}{\partial y^2} - \lambda_1\left(u^2\frac{\partial^2 u}{\partial x^2} + v^2\frac{\partial^2 u}{\partial y^2} + 2uv\frac{\partial^2 u}{\partial x\partial y}\right) - \frac{v}{K}u$$

$$-\frac{\sigma B^2}{\rho}u + g[\beta_T(T - T_\infty) + \beta_C(C - C_\infty)]. \tag{2}$$

Energy Equation:

$$u\frac{\partial T}{\partial x} + v\frac{\partial T}{\partial y} = \alpha_m \frac{\partial^2 T}{\partial y^2} + \frac{D_e K_T}{C_s C_p}\frac{\partial^2 C}{\partial y^2} + \tau\left[D_B \frac{\partial C}{\partial y}\frac{\partial T}{\partial y} + \frac{D_T}{T_\infty}\left(\frac{\partial T}{\partial y}\right)^2\right]. \tag{3}$$

Concentration Equation:

$$u\frac{\partial C}{\partial x} + v\frac{\partial C}{\partial y} = \frac{D_e K_T}{T_m}\frac{\partial^2 T}{\partial y^2} + D_B \frac{\partial^2 C}{\partial y^2} + \frac{D_T}{T_\infty}\frac{\partial^2 T}{\partial y^2} - K_1(C - C_\infty). \tag{4}$$

The boundary conditions of equations (1)-(4) are given as follows:

$$u = u_w(x) = ax, \; v = -v_0, \; T = T_w(x) = T_\infty + bx,$$

$$C = C_w(\text{x}) = C_\infty + cx, \qquad\qquad \text{at} \quad y = 0 .$$

$$u \to 0, \; \frac{\partial u}{\partial y} \to 0, \; T \to T_\infty, C \to C_\infty, \qquad \text{as} \quad y \to \infty. \tag{5}$$

Here, u and v are velocity components along x and $y-$axes respectively. Also, $D_B, T,$ $C, g, D_T, \alpha_m, \beta_T, \lambda_1, \tau = \frac{(\rho d)_p}{(\rho d)_f}$ and K_1 are Brownian motion coefficient, fluid temperature, nano particle concentration, gravitational acceleration, thermophoretic diffusion coefficient, thermal diffusivity, coefficient of thermal expansion, relaxation time, ratio of effective heat capacity of the nanoparticle to the fluid and chemical reaction parameter respectively. Further, $a > 0$ and $c > 0$ are positive constants. However, $b > 0$ denotes heated plate $(T_w > T_\infty)$ and for a cooled surface $(T_w < T_\infty)$.

We now introduce the following relations for $u, \; \theta$ and φ as follows:

$$u = \frac{\partial \psi}{\partial y}, \;\; v = -\frac{\partial \psi}{\partial x}, \;\; \theta = \frac{T - T_\infty}{T_w - T_\infty} \text{ and } \varphi = \frac{C - C_\infty}{C_w - C_\infty}, \tag{6}$$

where ψ is the stream function of the flow.

Using equation (6), equations (2)-(4) can be written as below:

$$\frac{\partial \psi}{\partial y}\frac{\partial^2 \psi}{\partial x \partial y} - \frac{\partial \psi}{\partial x}\frac{\partial^2 \psi}{\partial y^2} = v\frac{\partial^3 \psi}{\partial y^3} - \lambda_1\left(\left(\frac{\partial \psi}{\partial y}\right)^2\frac{\partial^3 \psi}{\partial x^2 \partial y} + \left(\frac{\partial \psi}{\partial x}\right)^2\frac{\partial^3 \psi}{\partial y^3} - 2\frac{\partial \psi}{\partial x}\frac{\partial \psi}{\partial y}\frac{\partial^3 \psi}{\partial y^2 \partial x}\right)$$
$$- \frac{v}{K}\frac{\partial \psi}{\partial y} - \frac{\sigma B^2}{\rho}\frac{\partial \psi}{\partial y} + g[\beta_T \theta(T_w - T_\infty) + \beta_C \varphi(C_w - C_\infty)] . \tag{7}$$

$$\frac{\partial \psi}{\partial y}\frac{\partial \theta}{\partial x} - \frac{\partial \psi}{\partial x}\frac{\partial \theta}{\partial y} = \alpha_m \frac{\partial^2 \theta}{\partial y^2} + \frac{D_m k_T}{C_s C_p}\frac{(C_w - C_\infty)}{(T_w - T_\infty)}\frac{\partial^2 \varphi}{\partial y^2} + \tau[D_B(C_w - C_\infty)\frac{\partial \psi}{\partial y}\frac{\partial \theta}{\partial y}$$
$$+ \frac{D_T}{T_\infty}\;(T_w - T_\infty)\left(\frac{\partial \theta}{\partial y}\right)^2] . \tag{8}$$

$$\frac{\partial \psi}{\partial y}\frac{\partial \varphi}{\partial x} - \frac{\partial \psi}{\partial x}\frac{\partial \varphi}{\partial y} = \frac{D_e K_T}{T_m}\left(\frac{(T_w - T_\infty)}{(C_w - C_\infty)}\right)\frac{\partial^2 \theta}{\partial y^2} + D_B \frac{\partial^2 \varphi}{\partial y^2} + \frac{D_T}{T_\infty}\left(\frac{(T_w - T_\infty)}{(C_w - C_\infty)}\right)\frac{\partial^2 \theta}{\partial y^2} - K_1\varphi. \tag{9}$$

Applications and Applied Mathematics: An International Journal (AAM), Vol. 15 [], Iss. 1, Art. 31

AAM: Intern. J., Vol. 15, Issue 1 (June 2020) 535

The boundary conditions equations (5) can be written as follows:

$$\frac{\partial \psi}{\partial y}(x,0) = ax, \quad \frac{\partial \psi}{\partial x}(x,0) = v_0, \quad \theta(x,0) = 1, \quad \varphi(x,0) = 1.$$

$$\frac{\partial \psi}{\partial y}(x,\infty) = 0, \quad \theta(x,\infty) = 0, \quad \varphi(x,\infty) = 0. \tag{10}$$

Scaling group of Transformations (Lie-group Analysis)

Firstly, we shall derive the similarity solutions using the Lie group method under which the non-linear differential equations (7)-(9) and the boundary conditions (10) are invariant. The simplified form of the Lie-group transformation, namely the scaling group of transformations given by Dessie et al. (2014) are of the form:

$$\Gamma: \ x^* = xe^{\varepsilon\alpha_1}, \ y^* = ye^{\varepsilon\alpha_2}, \ \psi^* = \psi e^{\varepsilon\alpha_3},$$

$$u^* = ue^{\varepsilon\alpha_4}, \ v^* = ve^{\varepsilon\alpha_5}, \ \theta^* = \theta e^{\varepsilon\alpha_6}, \ \varphi^* = \varphi e^{\varepsilon\alpha_7}, \tag{11}$$

where $\alpha_1, \alpha_2, \alpha_3, \alpha_4, \ \alpha_5, \alpha_6$ and α_7 are transformation parameters.

Equation(11) may be considered as a point-transformation which transforms coordinates $(x, y, \psi, u, v, \theta, \varphi)$ to the coordinates $(x^*, y^*, \psi^*, u^*, v^*, \theta^*, \varphi^*)$. Substituting equation (11) into (7) - (9) to obtain

$$e^{\varepsilon(\alpha_1+2\alpha_2-2\alpha_3)}\left(\frac{\partial\psi^*}{\partial y^*}\frac{\partial^2\psi^*}{\partial x^*\partial y^*} - \frac{\partial\psi^*}{\partial x^*}\frac{\partial^2\psi^*}{\partial y^{*2}}\right) = v e^{\varepsilon(3\alpha_2-\alpha_3)}\frac{\partial^3\psi^*}{\partial y^{*3}}$$
$$-\lambda_1 e^{\varepsilon(2\alpha_1+3\alpha_2-3\alpha_3)}\left(\left(\frac{\partial\psi^*}{\partial y^*}\right)^2\frac{\partial^3\psi^*}{\partial x^{*2}\partial y^*} + \left(\frac{\partial\psi^*}{\partial x^*}\right)^2\frac{\partial^3\psi^*}{\partial y^{*3}} + \frac{\partial\psi^*}{\partial x^*}\frac{\partial\psi^*}{\partial y^*}\frac{\partial^3\psi^*}{\partial y^{*2}\partial x^*}\right)$$
$$-\frac{v}{K}e^{\varepsilon(\alpha_2-\alpha_3)}\frac{\partial\psi^*}{\partial x^*} - \frac{\sigma B^2}{\rho}e^{\varepsilon(\alpha_2-\alpha_3)}\frac{\partial\psi^*}{\partial x^*} + g[\beta_T\theta^*e^{-\varepsilon\alpha_6}(T_w - T_\infty)$$
$$+ \ \beta_C\varphi^*e^{-\varepsilon\alpha_7}(C_w - C_\infty)]. \tag{12}$$

$$e^{\varepsilon(\alpha_1+\alpha_2-\alpha_3-\alpha_6)}\left(\frac{\partial\psi^*}{\partial y^*}\frac{\partial\theta^*}{\partial x^*} - \frac{\partial\psi^*}{\partial x^*}\frac{\partial\theta^*}{\partial y^*}\right) = \alpha_m\,e^{\varepsilon(2\alpha_2-\alpha_6)}\frac{\partial^2\theta^*}{\partial y^{*2}}$$
$$+\frac{D_m k_T}{C_S C_p}\frac{(C_w-C_\infty)}{(T_w-T_\infty)}\,e^{\varepsilon(2\alpha_2-\alpha_7)}\frac{\partial^2\varphi^*}{\partial y^{*2}} + \tau[D_B(C_w - C_\infty)\,e^{\varepsilon(2\alpha_2-\alpha_6-\alpha_7)}\frac{\partial\psi^*}{\partial y^*}\frac{\partial\theta^*}{\partial y^*}$$
$$+\frac{D_T}{T_\infty}(T_w - T_\infty)\,e^{\varepsilon(2\alpha_2-2\alpha_6)}\left(\frac{\partial\theta^*}{\partial y^*}\right)^2]. \tag{13}$$

$$e^{\varepsilon(\alpha_1+\alpha_2-\alpha_3-\alpha_7)}\left(\frac{\partial\psi^*}{\partial y^*}\frac{\partial\varphi^*}{\partial x^*} - \frac{\partial\psi^*}{\partial x^*}\frac{\partial\varphi^*}{\partial y^*}\right) = \frac{D_e K_T}{T_m}\left(\frac{(T_w-T_\infty)}{(C_w-C_\infty)}\,e^{\varepsilon(2\alpha_2-2\alpha_6)}\frac{\partial^2\theta^*}{\partial y^{*2}}\right)$$
$$+D_B e^{\varepsilon(2\alpha_2-\alpha_7)}\frac{\partial^2\varphi^*}{\partial y^{*2}} + \frac{D_T}{T_\infty}\left(\frac{(T_w-T_\infty)}{(C_w-C_\infty)}\right)\,e^{\varepsilon(2\alpha_2-2\alpha_6)}\frac{\partial^2\theta^*}{\partial y^{*2}} - K_1\varphi^*e^{-\varepsilon\alpha_7}. \tag{14}$$

The boundary conditions become:

$$y = 0; \ u^* e^{-\varepsilon\alpha_4} = ax^* e^{-\varepsilon\alpha_1}, v^* e^{-\varepsilon\alpha_5} = -\mathrm{v}_0, \theta^* e^{-\varepsilon\alpha_6} = 1, \varphi^* e^{-\varepsilon\alpha_7} = 1.$$

$$y \to \infty; \ u^* e^{-\varepsilon\alpha_4} = 0, \ \ \theta^* e^{-\varepsilon\alpha_6} = 0, \ \varphi^* e^{-\varepsilon\alpha_7} = 0. \tag{15}$$

However, the system of equations (12)-(15) remains invariant under the group of transformation Γ, if the following relations hold:

$$\alpha_1 + 2\alpha_2 - 2\alpha_3 = 3\alpha_2 - \alpha_3 = 2\alpha_1 + 3\alpha_2 - 3\alpha_3 = \alpha_2 - \alpha_3 = -\alpha_6$$
$$= -\alpha_7.$$
$$\alpha_1 + \alpha_2 - \alpha_3 - \alpha_6 = 2\alpha_2 - \alpha_6 = 2\alpha_2 - \alpha_7 = 2\alpha_2 - \alpha_6 - \alpha_7$$
$$= 2\alpha_2 - 2\alpha_6.$$
$$\alpha_1 + \alpha_2 - \alpha_3 - \alpha_7 = 2\alpha_2 - \alpha_6 = 2\alpha_2 - \alpha_7 = -\alpha_7.$$

From boundary conditions, we have:

$$-\alpha_4 = -\alpha_1, \ -\alpha_5 = 0.$$

This relation gives us the following:

$$\alpha_1 = \alpha_3 = \alpha_4 = \alpha_6 = \alpha_7, \ \ \ \alpha_2 = \alpha_5 = 0.$$

Thus, the set Γ reduces to a one parameter group transformation as below:

$$\Gamma: \ \ x^* = x e^{\varepsilon\alpha_1}, \ y^* = y, \ \ \psi^* = \psi e^{\varepsilon\alpha_1},$$
$$u^* = u e^{\varepsilon\alpha_1}, \ v^* = v, \ \theta^* = \theta e^{\varepsilon\alpha_1}, \ \varphi^* = \varphi e^{\varepsilon\alpha_1}. \tag{16}$$

Expanding by Taylor's method in powers of ε and keeping terms up to the order ε, we obtain

$$x^* - x = x\varepsilon\alpha_1, \ y^* - y = 0, \psi^* - \psi = \psi\varepsilon\alpha_1, \ u^* - u = u\varepsilon\alpha_1,$$
$$v^* - v = 0, \ \ \theta^* - \theta = \theta\varepsilon\alpha_1, \ \varphi^* - \varphi = \varphi\varepsilon\alpha_1.$$

After differentials, we have,

$$\frac{dx}{\alpha_1 x} = \frac{dy}{0} = \frac{d\psi}{\psi\alpha_1} = \frac{d\theta}{\theta\alpha_1} = \frac{d\varphi}{\varphi\alpha_1}. \tag{17}$$

Solving the above equation, we obtain

$$\eta = y, \ \ \psi = xF(\eta), \theta = xh(\eta), \ \varphi = xS(\eta). \tag{18}$$

Applications and Applied Mathematics: An International Journal (AAM), Vol. 15 [], Iss. 1, Art. 31

AAM: Intern. J., Vol. 15, Issue 1 (June 2020) 537

Using these transformation equations (12) - (14) become:

$$F'^2 - FF'' = vF''' - \lambda_1 F^2 F''' + 2\lambda_1 FF'F'' - \frac{v}{K}F' - \frac{\sigma B_0^2}{\rho}F'$$
$$+ g\beta_T(T_w - T_\infty)\theta + g\beta_C(C_w - C_\infty)\varphi. \tag{19}$$

$$F'h - Fh' = \alpha_m h'' + \frac{D_m k_T}{C_s C_p}\frac{(C_w - C_\infty)}{(T_w - T_\infty)}S'' + \tau[D_B(C_w - C_\infty)xh'S'$$
$$+ \frac{D_T}{T_\infty}(T_w - T_\infty)h'^2]. \tag{20}$$

$$F'S - FS' = D_B S'' + \frac{D_m k_T}{T_m}\frac{(T_w - T_\infty)}{(C_w - C_\infty)}h'' + \frac{D_T}{T_\infty}\left(\frac{(T_w - T_\infty)}{(C_w - C_\infty)}\right)h'' - K_1\varphi. \tag{21}$$

The boundary conditions are transformed to the following form:

$$F' = a, \; F = s, \; \theta = 1, \; \varphi = 1 \quad \text{at} \quad \eta = 0.$$

$$F' \to 0, \; F'' \to 0, \; \theta \to 0, \; \varphi \to 0 \quad \text{as } \eta \to \infty. \tag{22}$$

Introducing the following transformations for η, F, h and S in equations (19)-(22),

$$\eta = v^\alpha a^\beta \eta^*, \; F = v^{\alpha'} a^{\beta'} F^*, \; h = v^{\alpha''} a^{\beta''}\theta^*, \; S = v^{\alpha'''} a^{\beta'''}\varphi^*,$$

we have:

$$\alpha' = \alpha = 1/2, \; \alpha'' = 0 = \alpha''', \; \beta' = -\beta = 1/2, \; \beta'' = 0 = \beta'''.$$

The equations (19)-(22) are transformed in to:

$$F^{*'^2} - F^*F^{*''} = F^{*'''} - \lambda_1 a F^* F^{*'''} + 2\lambda_1 a F^* F^{*'} F^{*''}$$
$$- \frac{v}{ka}F^{*'} - F^{*'} + \frac{g\beta_T(T_w - T_\infty)}{a^2}\theta^* + \frac{g\beta_C(C_w - C_\infty)}{a^2}\varphi^*. \tag{23}$$

$$F^{*'}\theta^* - F^*\theta^{*'} = \frac{\alpha_m}{v}\theta^{*''} + \frac{D_m k_T}{C_s C_p}\frac{(C_w - C_\infty)}{(T_w - T_\infty)v}\varphi^{*''}$$
$$+ \tau[\frac{D_B(C_w - C_\infty)}{v}\theta^{*'}\varphi^{*'} + \frac{D_T}{vT_\infty}(T_w - T_\infty)]\theta^{*'^2}. \tag{24}$$

$$F^{*'}\varphi^* - F^*\varphi^{*'} = \frac{D_B}{v}\varphi^{*''} + \frac{D_m k_T}{vT_m}\frac{(T_w - T_\infty)}{(C_w - C_\infty)}\theta^{*''}$$
$$+ \frac{D_T}{vT_\infty}\left(\frac{(T_w - T_\infty)}{(C_w - C_\infty)}\right)\theta^{*''} - \frac{K_1}{a}\varphi^*. \tag{25}$$

Let $F^* = f$, $\theta^* = \theta$ and $\varphi^* = \varphi$ equations (23)-(25) finally become:

$$f''' + ff'' - f'^2 + \beta(2ff'f'' - f^2f''') - (\gamma + M)f' + \lambda(\theta + N\varphi) = 0. \tag{26}$$

$$\frac{1}{Pr}\theta'' + f\theta' - \theta f' + D_f\varphi'' + Nb\theta'\varphi' + Nt\theta'^2 = 0. \tag{27}$$

$$\varphi'' + PrLe(f\varphi' - \varphi f') + SrLe\theta'' + \frac{Nt}{Nb}\theta'' - LeK\varphi = 0. \tag{28}$$

The corresponding boundary conditions take the form:

$$f' = 1, \quad f = s, \quad \theta = 1, \quad \varphi = 1 \quad \text{at } \eta = 0.$$
$$f' = 0, \quad \theta = 0, \quad \varphi = 0 \quad \text{at } \eta \to \infty, \tag{29}$$

with $M, Nt, Le = \frac{\alpha_m}{D_B}, Nb, D_f, Pr = \frac{v}{\alpha_m}, \lambda, \beta(\geq 0), N, \gamma, Sr$ and K are magnetic parameter, thermophores parameter, Lewis number, Brownian motion parameter, DuFour number, Prandtl number, dimensionless mixed convection parameter, Deborah parameter, dimensionless concentration buoyancy parameter, dimensionless porosity parameter, Soret number and chemical reaction parameter respectively. We define these parameters as follows:

$$M = \frac{\sigma B_0^2}{\rho a}, \lambda = \frac{g\beta_T}{a^2} = \frac{g\beta_T(T_w - T_\infty)x}{u_w^2} = \frac{Gr_x}{Re_x^2}, N = \frac{\beta_C(C_w - C_\infty)}{\beta_T(T_w - T_\infty)}, \gamma = \frac{v}{ka}, \beta = \lambda_1,$$
$$D_f = \frac{D_m k_T}{C_s C_p}\frac{(C_w - C_\infty)}{(T_w - T_\infty)v}, \quad Nb = \tau\left[\frac{D_B(C_w - C_\infty)}{v}\right], \quad Nt = \tau\left[\frac{D_T}{vT_\infty}(T_w - T_\infty)\right], \quad K = \frac{K_1}{a}. \tag{30}$$

Here, $Re_x = \frac{u_w x}{v}, Gr_x = g\beta_T(T_w - T_\infty)x^3/v^2$ are the local Reynolds and Grashof numbers. Moreover, $\lambda > 0, \lambda < 0$ and $\lambda = 0$ depict supporting flow (heated plate), opposing flow (cooled plate) and forced convection flow. Moreover, N can take positive values ($N > 0$) and negative values ($N < 0$) with $N = 0$ (in the absence of mass transfer).

The quantities of physical interest in this problem are the local skin friction coefficient, the local Nusselt number and the local Sherwood numbers, which are defined by:

$$C_f = \frac{\tau_w}{\rho u_w^2} = 2Re_x^{\frac{-1}{2}}f''(0), Nu = \frac{xq_w}{k(T_w - T_\infty)} = -Re_x^{\frac{1}{2}}\theta'(0), Sh = \frac{xm_w}{D_m(C_w - C_\infty)} = -Re_x^{\frac{1}{2}}\varphi'(0), \tag{31}$$

where

$$\tau_w = \mu(1 + \beta)\left(\frac{\partial u}{\partial y}\right)(x, 0), q_w = -k\left(\frac{\partial T}{\partial y}\right)(x, 0) \text{ and } m_w = -D_m\left(\frac{\partial u}{\partial y}\right)(x, 0). \tag{32}$$

3. Method of Solution

The set of coupled non-linear ordinary differential equations (26)-(28) together with boundary conditions (29) are solved numerically by using Runge-Kutta fourth order technique along with

Applications and Applied Mathematics: An International Journal (AAM), Vol. 15 [], Iss. 1, Art. 31

AAM: Intern. J., Vol. 15, Issue 1 (June 2020) 539

shooting method. First of all, the higher order non-linear differential equations (26) and (27) are converted into simultaneous linear differential equation of first order and they are further transformed into initial value problem by applying the shooting technique. Once the problem is reduced to initial value problem, then it is solved by Runge-Kutta fourth order technique. The step size $\Delta\eta = 0.001$ is used to obtain the numerical solution with six decimal accuracy as criterion of convergence. The above mentioned third order and second order equations are written in terms of first order equations as follows:

$$f_1 = f, \ f_2 = f', f_3 = f'', f_4 = \theta, f_5 = \theta', f_6 = \varphi \ f_7 = \varphi'.$$

The coupled higher order differential equations and the boundary conditions may be transformed to seven equivalent first order differential equations and boundary conditions, respectively, as given below:

$$f_1' = \ f_2,$$
$$f_2' = f_3,$$
$$f_3' = -f_1 f_3 + f_2{}^2 - 2\beta f_1 \ f_2 f_3 + \left(\gamma + M\right) f_2 - \frac{f_4 + N f_6}{1 - \beta f_1{}^2},$$
$$f_4' = f_5,$$
$$f_5' = \frac{-\mathrm{Pr} f_1 f_5 + \mathrm{Pr} f_2 f_4 + \mathrm{Pr} Df[\mathrm{Pr} Le(f_1 f_7 - f_6 f_2)] - \mathrm{Pr} N b f_5 f_7 - \mathrm{Pr} N t f_5{}^2}{\left(1 - \mathrm{Pr} Df SrLe - \mathrm{Pr} Df \dfrac{Nt}{Nb}\right)},$$
$$f_6' = f_7,$$
$$f_7' = -\mathrm{Pr} Le[f_1 f_7 - f_2 f_6 - K f_6] \ - \left(SrLe + \frac{Nt}{Nb}\right)$$
$$\mathrm{X}\left(\frac{-\mathrm{Pr} f_1 f_5 + \mathrm{Pr} f_2 f_4 + \mathrm{Pr} Df[\mathrm{Pr} Le(f_1 f_7 - f_6 f_2)] - \mathrm{Pr} N b f_5 f_7 - \mathrm{Pr} N t f_5{}^2}{\left(1 - \mathrm{Pr} Df SrLe - \mathrm{Pr} Df \frac{Nt}{Nb}\right)}\right)$$

$$(33)$$

A prime denotes the differentiation with respect to η and the boundary conditions are

$$f_1(0) = s, \ f_2(0) = 1 \ , f_4(0) = 1, f_6(0) = 1,$$

$$f_2(\infty) = 0 \ , f_4(\infty) = 0, \ f_6(\infty) = 0. \tag{34}$$

In order to numerically solve this system of equations (33) using Runge-Kutta method, seven initial conditions are required but two initial conditions in f, one initial condition in each of θ and φ are known. However, the values of f, θ and φ are known at $\eta \rightarrow \infty$. Thus, these end conditions are utilized to produce unknown initial conditions at $\eta = 0$ by using shooting technique. The most important step of this scheme is to choose the appropriate finite value of $\eta\infty$. Thus to estimate the value of $\eta\infty$, the solution starts with some initial guess value and solve the boundary value problem consisting of equations.(26)-(28) to obtain $f''(0), \theta'(0)$ and $\varphi'(0)$. The solution process is repeated with another larger value of $\eta\infty$ until two successive values of $f''(0)$, $\theta'(0)$ and $\varphi'(0)$ differ only after desired significant digit. The last value η_∞ is taken as the finite value of the limit $\eta\infty$ for the particular set of physical parameters for determining velocity,

temperature and concentration, respectively, are $f'(\eta)$, $\theta(\eta)$ and $\varphi(\eta)$ in the boundary layer. After getting all the initial conditions, this system of simultaneous equations is solved using fourth order Runge-Kutta integration scheme. In this study, it has been considered the iterative process, which is terminated to converge when the difference between two successive values are reached 10^{-6}.

4. Results and Discussion

In order to get a clear insight of the physical problem, numerical computations have been carried out using fourth order Runge-Kutta method along with shooting technique for various values of different parameters such as thermophoresis Nt, Lewis parameter Le, Prandtl number Pr, magnetic parameter M, chemical reaction parameter K, Brownian motion parameter Nb, velocity suction parameter s, Dufour number Df, dimensionless mixed convection parameter λ, Deborah number β, dimensionless concentration buoyancy parameter N, dimensionless porosity parameter γ and Soret number Sr. In order to verify the validity and accuracy of the present analysis, the results for the heat transfer $-\theta'(0)$ and mass transfer $-\varphi'(0)$ were compared with those reported by M. Ramzan et al. (2016). The comparison in the above cases is found to be in excellent agreement as shown in Table 1. The values of local skin-friction coefficient, temperature gradient and mass transfer rate are tabulated in Table 2. It is noted that from Table 2, both the values of temperature gradient $-\theta'(0)$ and the Sherwood number $-\varphi'(0)$ decrease with increasing of magnetic parameter M but skin-friction $-f''(0)$ increases. From the table, it is observed that the temperature gradient $-\theta'(0)$ decreases but skin-friction $-f''(0)$ as well as the Sherwood number $-\varphi'(0)$ increase with the increase of the chemical reaction rate parameter K. The increase of suction parameter s is to increase the skin–friction coefficient $-f''(0)$, the temperature gradient $-\theta'(0)$ and the Sherwood number $-\varphi'(0)$ as it is noted from the table. Both the skin-friction coefficient $-f''(0)$ and the mass flow rate $-\varphi'(0)$ decrease with the increase of DuFour number D_f but the Nusselt number (temperature gradient) $-\theta'(0)$ increases. From the same table, it is clearly noted that the effect of Lewis number Le increases both the skin-friction coefficient $-f''(0)$ and the mass flow rate $-\varphi'(0)$ but decreases temperature gradient $-\theta'(0)$. It is witnessed that for the increasing value of the dimensionless concentration buoyancy parameter, $N < 0$, the skin–friction coefficient $-f''(0)$ increases whereas the temperature gradient $-\theta'(0)$ and the Sherwood number $-\varphi'(0)$ decrease. But for the increase values of the positive values of N, the skin–friction coefficient $-f''(0)$ decreases whereas the temperature gradient $-\theta'(0)$ and the Sherwood number $-\varphi'(0)$ increase. Lastly, it is noticed that the skin–friction coefficient $-f''(0)$ and the temperature gradient $-\theta'(0)$ decreases but the Sherwood number $-\varphi'(0)$ increases with the increase of the Brownian motion parameter Nb.

The dimensionless velocity, temperature and concentration profiles are shown graphically in the Figures 1a-6b for the different flow parameters. For different values of the magnetic parameter M, the velocity and the temperature profiles are plotted in Figure 1a and 1b respectively. From Figure 1a, it is clear that an increase in the magnetic parameter M leads to a fall in the velocity. The effects of the magnetic parameter to increase the temperature profiles are noticed from Figure 1b. The presence of Lorentz force retards the force on the velocity field and therefore the velocity profiles decreases with the effect of magnetic parameter. This force has the tendency to slow down the fluid motion and the resistance offered to the flow. Therefore, it is possible for the

Applications and Applied Mathematics: An International Journal (AAM), Vol. 15 [], Iss. 1, Art. 31

AAM: Intern. J., Vol. 15, Issue 1 (June 2020)   541

increase in the temperature. The variations of the fluid velocity profiles and concentration profiles with chemical reaction K are shown in Figure 2a & 2b respectively from which it is observed both the velocity and concentration profiles decrease with the increase of the chemical reaction. Figures 3a-3c display the effects of suction parameter s on velocity, temperature and concentration profiles. It is observed that the effect of suction parameter is to reduce all those profiles as shown in the figures. Figure 4 depicts the effect of DuFour parameter on temperature profiles. As the DuFour parameter increases, the energy or temperature profiles increases. The Dufour number denotes the contribution of the concentration gradients to the thermal energy flux in the flow. It can be seen that an increase in the Dufour number causes a rise in temperature. Figure 5a and Figure 5b illustrate the effects of Brownian motion parameter Nb on temperature and concentration profiles. This parameter reduces the temperature profiles whereas it enhances the concentration profiles. In Figure 6a and 6b, the effect of Lewis number Le on fluid velocity and concentration profiles exhibited, respectively. It is clearly shown that this parameter reduces both velocity and concentration profiles. By definition, Lewis number is the ratio of thermal diffusivity to mass diffusivity. Increasing the value of Le is the same as maximizing thermal boundary layer thickness at the expense of minimizing concentration boundary layer thickness.

5. Conclusion

In this work, MHD mixed convective flow of Maxwell nanofluid past a porous vertical stretched surface in presence of chemical reaction is investigated. The resulting partial differential equations, which describe the problem, are transformed in to ordinary differential equations by using scaling group transformation (Lie group analysis) and then solved by numerically by fourth order Runge-Kutta method along with shooting technique. Velocity, temperature and concentration profiles are presented graphically and analyzed. The findings of the numerical results can be summarized as follows:

i)   An increase in the magnetic parameter leads to a fall in the velocity and rise in the temperature profiles.

ii)   It is found that both the velocity and concentration profiles decrease with the increase of the chemical reaction.

iii)   It is observed that the effects of suction parameter are to reduce the velocity, temperature and concentration profiles.

iv)   It is also found that the temperature profiles increase whereas the concentration profiles decrease with the increase of Brownian motion parameter.

REFERENCES

Abbasi, F.M., Mustafa, M., Shehzad, S.A., Alhuthali, M.S. And Hayat, T. (2015). Analytical study of Cattaneo-christov heat flux model for the boundary layer flow of Oldroyd-B fluid, Chin Phys B, Vol.25(1):014701.

Ahmad, M., Ahmad, I. and Sajid, M. (2016). Magnetohydrodynamic time-dependent three dimensional flow of Maxwell fluid over a stretching surface through porous space with variable thermal conditions, J Braz Soc Mech Sci, pp.1–12.

Awais, M., Hayat, T., Irum, S. and Alsaedi, A. (2015). PLoS ONE10(6): e0129814.

Bahttacharyya, K.and Layek, G.C. (2010). Chemically reactive solute distribution in MHD boundary layer flow over a permeable stretching sheet with suction or blowing, *Chem. Eng. Commun, Vol.*197, pp.1527-1540.

Bhattacharyya, K., Hayat, T.and Alsaedi, A. (2013). Effect of thermal radiation on Casson fluid and heat transfer over an unsteady stretching surface subjected to suction/blowing, Chin. Phys. B, Vol. 22, 024702.

Bahttacharyya, K., Mukhopadhyay, S. and Layek, G.C. (2013). Unsteady MHD boundary layer flow with diffusion and first order chemical reaction over a permeable stretching sheet with suction or blowing, *Chemical Engineering Communications.* 200(3), pp.379.

Buongiorno, J. (2006). Convective transport in nanofluids, Heat Transf, Vol.128 (3), pp.240–250**.** Dessie, H. and N. Kishan, N. (2014). MHD effects on heat transfer over stretching sheet embeded in porous medium with variable viscosity, viscous dissipation and heat source/sink, Ain Shams Engineering J., Vol. 5(3), pp.967-977**.**

Desssie, H. and Kishan, N. (2014). Scaling group analysis on MHD free convective heat and mass transfer over stretching surface with suction/injection, heat source/sink considering viscous dissipation and chemical reaction effects, Applications and Applied mathematics, An International Journal (AAM), Vol.9(2), pp.553-572.

Ellahi, R., Hassan, M., Zeeshan, A. (2015). Shape effects of nanosize particles in CuHO nanofluid on entropy generation, Int J Heat Mass Transf, Vol.81, pp.449–456.

Eshetu, H. and Shanker, B. (2015). Boundary layer flow of nanofluids over a moving surface in the presence of thermal radiation, viscous dissipation and chemical reaction, Applications and Applied mathematics, An International Journal (AAM), Vol.10(2), pp.952-969.

Hady, F.M., Ibrahim, F. S, Abdel-Gaied, S.M. and Eid, M.R. (2012). Radiation effect on viscous flow of a nanofluid and heat transfer over a non-linearly stretching sheet, Nanoscale *Research Letters, Vol.* 7**.**

Harris J. (1977). Rheology and non-Newtonian flow. London: Longman, pp.28.

Hayat, T., Abbas, Z. and Sajid, M. (2009). MHD stagnation point flow of an upper convicted Maxwell fluid over stretching surface, Chaos Solitons Fract, Vol.39, pp. 840–848.

Ibrahim, W. and UlHaq, R. (2015). Magnetohydrodynamic (MHD) stagnation point flow of nanofluid past a stretching sheet with convective boundary conditions, J. Braz. Soc. Mech. Sci. Eng**.,** http://dx.doi.org/10.1007/s40430-015-0347-z.

KiranKumar, R., Raju, V. Durgaparasad, P. and Varma, S. (2016). Heat and mass transfer in MHD micropolar fluid in the presence of Diffusion thermo and chemical reaction, Applications and Applied Mathematics: An international Journal (AAM), Vol.11 (2), pp.704-721.

Kumari, M. and Nath, G. (2009). Steady mixed convection stagnation point flow of upper Maxwell fluids with magnetic field, Int J Non-Linear Mech, Vol.44 (10), pp.1048–1055.

Makinde. O.D. and Aziz, A. (2011). Boundary layer flow of a nanofluid past a stretching sheet with convective boundary condition, Int. J. Therm. Sci., Vol.50, pp.1326–1332.

Makinde, O.D., Khan, W.A., Culham, J. A. (2016). MHD variable viscosity reacting flow over a convectively heated plate in a porous medium with thermophoresis and radiative heat transfer, Int J Heat Mass Transf, Vol.93, pp.595–604.

Nadeem, S., Haq, R. and Khan, ZH. (2014). Numerical study of MHD boundary layer flow of a Maxwell fluid past a stretching sheet in the presences of nanoparticles, J Taiwan Inst Chem Eng, Vol.45 (1), pp.121–126.

Applications and Applied Mathematics: An International Journal (AAM), Vol. 15 [], Iss. 1, Art. 31

AAM: Intern. J., Vol. 15, Issue 1 (June 2020)   543

Noor, N.F.M, UlHaq, R., Nadeem, S. and Hashim, I. (2015). Mixed convection stagnation flow of a micropolar nanofluid along a vertically stretching surface with slip effects, Meccanica, Vol.50, pp.2007-2022.

Qayyum, A., Hayatc, T., Alhuthali, M.S. and Malaikah, H.M.(2014). Newtonian heating effects in three-dimensional flow of viscoelastic fluid, Chin Phys B, Vol.23, 054703.

Ramesh, G.K., and Gireesha, B.J. (2014). Influence of heat source/sink on a Maxwell fluid over a stretching surface with convective boundary condition in the presence of nanoparticles, Ain Shams Eng.J.,Vol.5(3), pp.991–998.

Ramesh, K. (2016). Influence of heat and mass transfer on peristaltic flow of a couple stress fluid through porous medium in the presence of inclined magnetic field in an inclined asymmetric channel, J Mol Liq, Vol. 219, pp.256–271.

Ramzan, M., Bilal, M., Chung, Jae Dong. and Farooq, U.(2016). Mixed convection flow of Maxwell nanofluid past a porous vertically stretched surface, Results in Physics. 6, pp.1072–1079.

Sadeghy, K., Najafi, A.H. and Saffari pour, M. (2005). Sakiadis flow of an upper convicted Maxwell fluid, Int J Non-Linear Mech, Vol.40, pp.1220–1228.

Shafique, Z., Mustafa, M. and Mushtaq, A. (2016). Boundary layer flow of Maxwell fluid in rotating frame with binary chemical reaction and activation energy, Results Phys, Vol.6, pp. 627–633.

Shehzad, S. A., Hayat, T. and Alsaedi, A. (2016). Three-dimensional MHD flow of Casson fluid in porous medium with heat generation, J Appl Fluid Mech, Vol.9 (1), pp.215–223.

Sheikholeslami, M., Ellahi, R., Ashorynejad, H.R., Domairry, G. and Hayat T. (2014). Effects of heat transfer in flow of nanofluids over a permeable stretching wall in a porous medium, J Comput Theor Nanosci, Vol.11 (2), pp.486–496.

UlHaq, R., Nadeem, S., Akbar, N.S. and Khan, Z.H. (2015). Buoyancy and radiation effect on stagnation point flow of micropolar nanofluid along a vertically convective stretching surface, IEEE Trans. Nanotechnol., ol.14(1), pp.42–50.

Yilmazoglu, M. Turk. and Pop, I. (2013). Exact analytical solutions for the flow and heat transfer near the stagnation point on a stretching /shrinking sheet in Jeffrey fluid, Int J Heat Mass Transf, Vol.57 (1), pp.82–88.

Zheng, I. Wang, L. and Zhang, X. (2011). Analytical solutions of unsteady boundary flow and heat transfer on a permeable stretching sheet with no-uniform heat source/sink, Commun. Nonlinear Sci. Numer. Simulat., Vol.16(2), pp.731-740.

APPENDIX

Table1: Comparison of $-\theta'(0)$ and $-\phi'(0)$ for some values of s, β, γ, λ, N and Pr for $Df = 0.1, Le = 1, Sr = 0.2, Nb = 0.8$ and $Nt = 0.1$.

s	B	γ	λ	N	Pr	Ramzanet et al. (2016)		Present study	
						$-\theta'(0)$	$-\phi'(0)$	$-\theta'(0)$	$-\phi'(0)$
0	0.1	2.0	1.0	1.0	1.0	0.71104	0.89301	0.71085	0.89367
0.3	0.1	2.0	1.0	1.0	1.0	0.79696	1.01679	0.79677	1.017180
0.5	0.1	2.0	1.0	1.0	1.0	0.85983	1.10661	0.85980	1.107100
0.9	0.1	2.0	1.0	1.0	1.0	0.99873	1.30359	0.998690	1.30360
0.5	0	2.0	1.0	1.0	1.0	0.86690	1.11816	0.86679	1.11891
0.5	0.2	2.0	1.0	1.0	1.0	0.85263	1.09559	0.85248	1.09653
0.5	0.4	2.0	1.0	1.0	1.0	0.83795	1.07326	0.83744	1.07685
0.5	0.1	0.5	1.0	1.0	1.0	0.91493	1.19556	0.91492	1.19666
0.5	0.1	1.0	1.0	1.0	1.0	0.89498	1.16286	0.84484	1.163250
0.5	0.1	1.5	1.0	1.0	1.0	0.87680	1.13337	0.87643	1.13395
0.5	0.1	2.0	0.5	1.0	1.0	0.81762	1.03883	0.81762	1.03956
0.5	0.1	2.0	0.8	1.0	1.0	0.84445	1.08202	0.84429	1.08336
0.5	0.1	2.0	1.2	1.0	1.0	0.87379	1.12906	0.87368	1.12969
0.5	0.1	2.0	1.0	-0.2	1.0	0.80842	1.02316	0.80837	1.02579
0.5	0.1	2.0	1.0	-0.1	1.0	0.81357	1.03149	0.81349	1.03399
0.5	0.1	2.0	1.0	0.5	1.0	0.84071	1.07596	0.84057	1.07728
0.5	0.1	2.0	1.0	1.0	0.7	0.77431	0.84566	0.77404	0.84831
0.5	0.1	2.0	1.0	1.0	1.2	0.88622	1.27852	0.886100	1.27889
0.5	0.1	2.0	1.0	1.0	1.5	0.89045	1.53416	0.89040	1.53428

Applications and Applied Mathematics: An International Journal (AAM), Vol. 15 [], Iss. 1, Art. 31

AAM: Intern. J., Vol. 15, Issue 1 (June 2020)   545

Table 2. The values of Skin-friction coefficient $f''(0)$, Nusselt number coefficient $-\theta'(0)$ and Sherwood number coefficient $-\varphi'(0)$ for different values of the flow parameters.

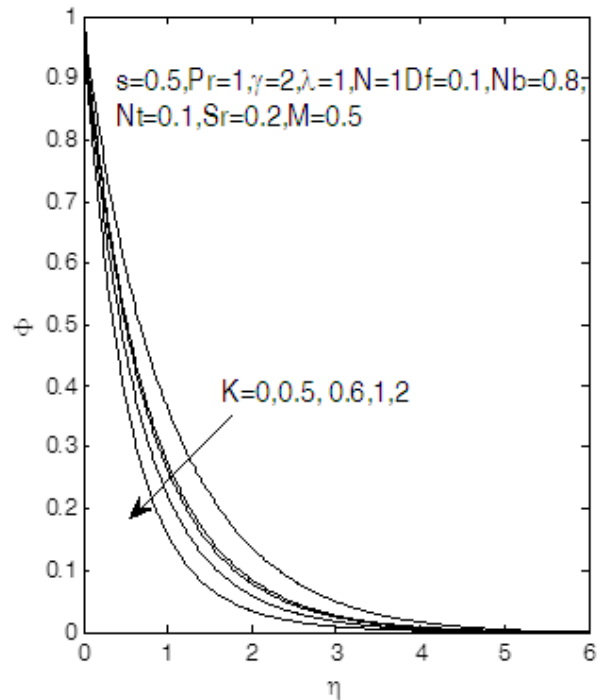| M	K	s	Df	Nb	Le	N	$-f''(0)$	$-\theta'(0)$	$-\phi'(0)$
0.5	0.5	0.5	0.1	0.8	1.0	1.0	1.48091	0.79743	1.37921
1.0	0.5	0.5	0.1	0.8	1.0	1.0	1.63651	0.78215	1.36601
1.5	0.5	0.5	0.1	0.8	1.0	1.0	1.78197	0.76807	1.35415
2.0	0.5	0.5	0.1	0.8	1.0	1.0	1.91931	0.75606	1.34381
0.5	0	0.5	0.1	0.8	1.0	1.0	1.4441	0.84439	1.08402
0.5	0.5	0.5	0.1	0.8	1.0	1.0	1.48091	0.79743	1.37922
0.5	0.6	0.5	0.1	0.8	1.0	1.0	1.48648	0.79064	1.42856
0.5	1.0	0.5	0.1	0.8	1.0	1.0	1.50533	0.76837	1.60614
0.5	2.0	0.5	0.1	0.8	1.0	1.0	1.53820	0.73185	1.96423
0.5	0.5	0	0.1	0.8	1.0	1.0	1.16008	0.64921	1.15885
0.5	0.5	0.3	0.1	0.8	1.0	1.0	1.33902	0.73389	1.28816
0.5	0.5	0.5	0.1	0.8	1.0	1.0	1.48091	0.79743	1.37921
0.5	0.5	0.9	0.1	0.8	1.0	1.0	1.83797	0.93963	1.57214
0.5	0.5	1.5	0.1	0.8	1.0	1.0	2.68017	1.18196	1.88539
0.5	0.5	0.5	0.0	0.8	1.0	1.0	1.48758	0.85776	1.36148
0.5	0.5	0.5	0.2	0.8	1.0	1.0	1.47418	0.73420	1.39779
0.5	0.5	0.5	0.4	0.8	1.0	1.0	1.46014	0.59807	1.43777
0.5	0.5	0.5	0.6	0.8	1.0	1.0	1.44559	0.44721	1.48208
0.5	0.5	0.5	1.0	0.8	1.0	1.0	1.41454	0.08951	1.58733
0.5	0.5	0.5	0.1	0.8	0.6	1.0	1.43325	0.89272	0.95367
0.5	0.5	0.5	0.1	0.8	1.2	1.0	1.49888	0.76164	1.57346
0.5	0.5	0.5	0.1	0.8	2.0	1.0	1.55035	0.65518	2.28561
0.5	0.5	0.5	0.1	0.8	3.0	1.0	1.59078	0.56023	3.10081
0.5	0.5	0.5	0.1	0.8	1.0	-0.5	1.99115	0.73908	1.33141
0.5	0.5	0.5	0.1	0.8	1.0	-0.2	1.88694	0.75220	1.34160
0.5	0.5	0.5	0.1	0.8	1.0	-0.1	1.85246	0.75639	1.34492
0.5	0.5	0.5	0.1	0.8	1.0	0.5	1.64810	0.77981	1.36411
0.5	0.5	0.5	0.1	0.8	1.0	1.5	1.31633	0.81363	1.39359
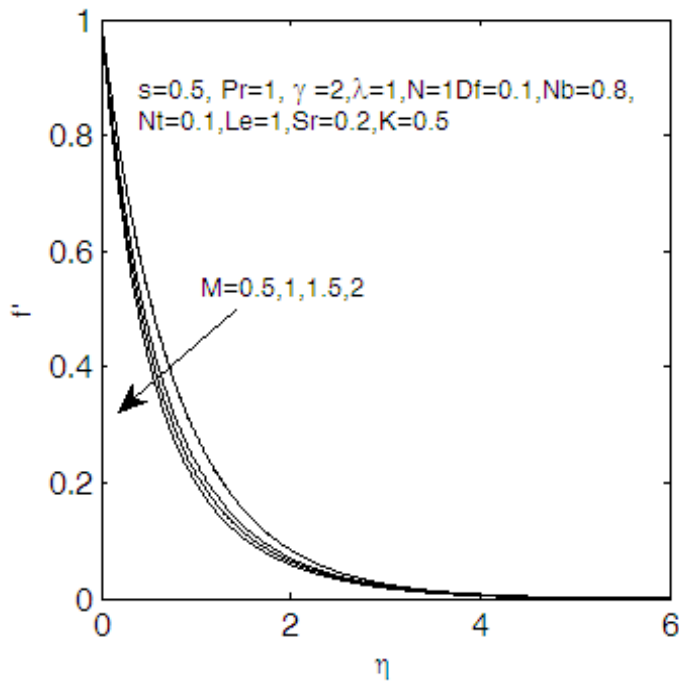
Figure1a. Effect of magnetic parameter M
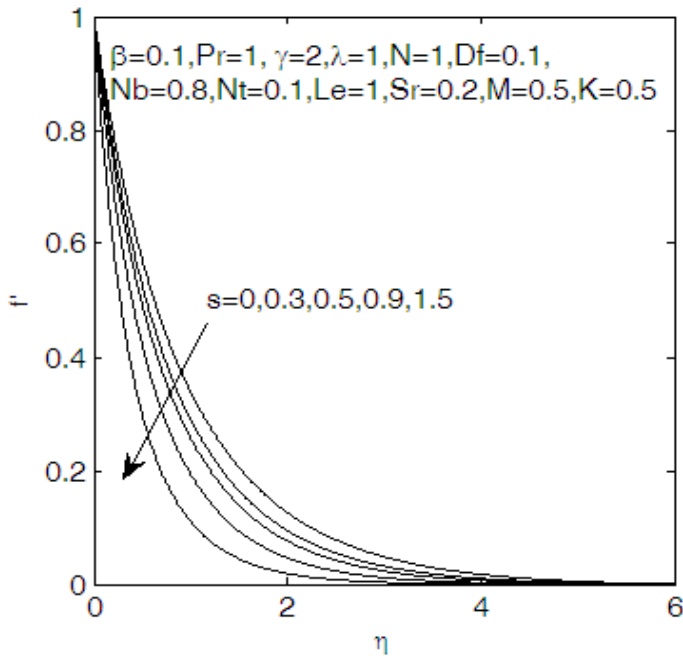 on velocity profiles
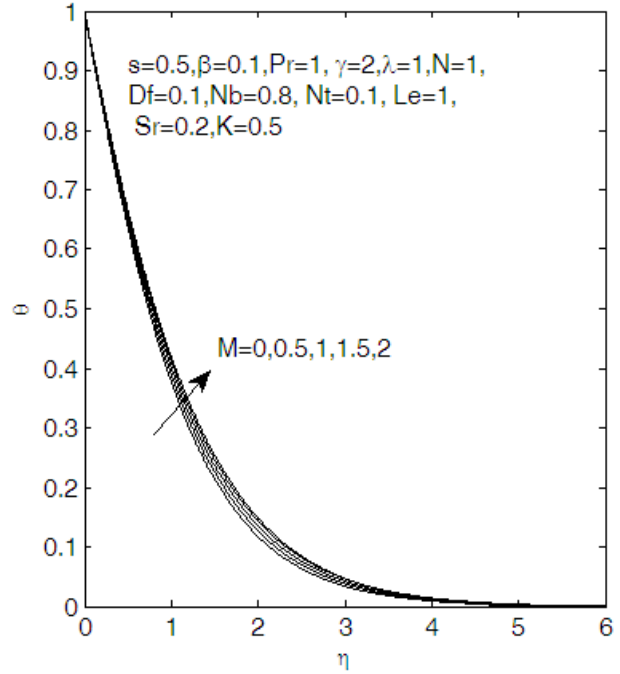
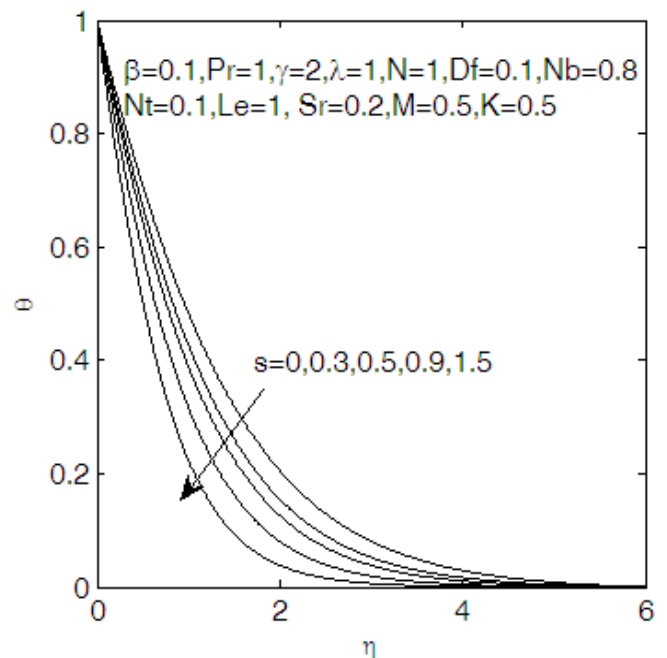**Figure1b.** Effect of M on Temperature profiles
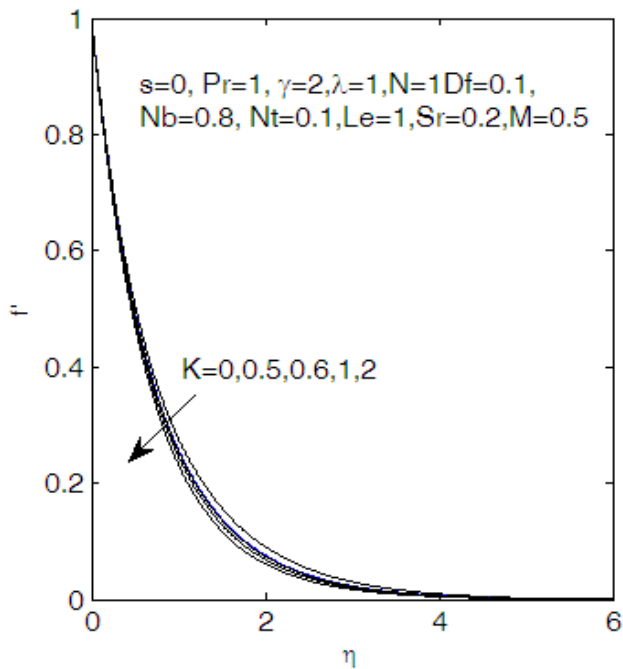
Figure2a. Effect of chemical reaction
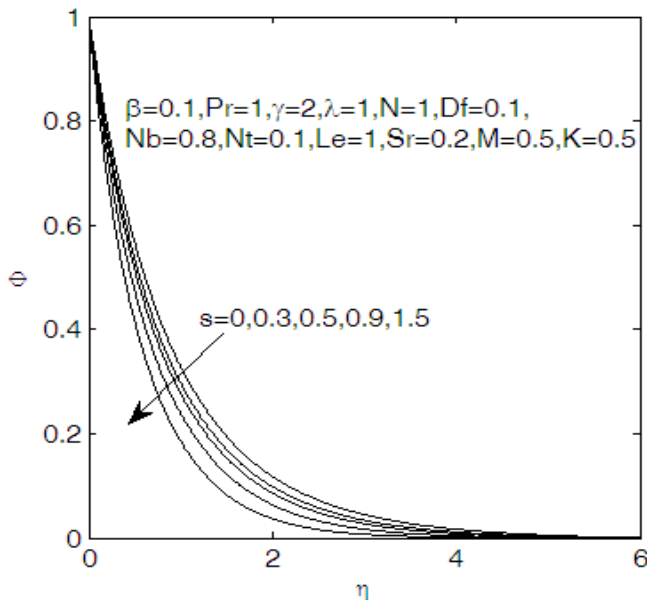 parameter K on velocity profiles

Figure 2b. Effect of chemical reaction
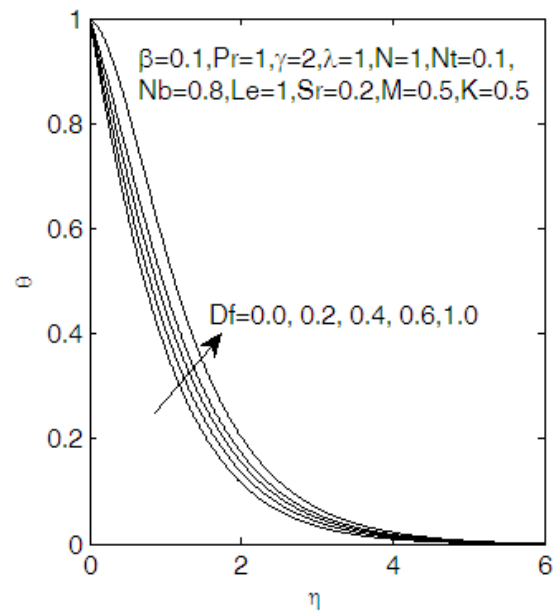 parameter K on concentration profiles

Applications and Applied Mathematics: An International Journal (AAM), Vol. 15 [], Iss. 1, Art. 31

AAM: Intern. J., Vol. 15, Issue 1 (June 2020)   547

β=0.1,Pr=1, γ=2,λ=1,N=1,Df=0.1,
Nb=0.8,Nt=0.1,Le=1,Sr=0.2,M=0.5,K=0.5

s=0,0.3,0.5,0.9,1.5

Figure 3a. Effect of suction parameter s
on velocity   profiles

β=0.1,Pr=1,γ=2,λ=1,N=1,Df=0.1,Nb=0.8
Nt=0.1,Le=1, Sr=0.2,M=0.5,K=0.5

s=0,0.3,0.5,0.9,1.5

Figure3b. Effect of suction parameter s
on temperature profiles

β=0.1,Pr=1,γ=2,λ=1,N=1,Df=0.1,
Nb=0.8,Nt=0.1,Le=1,Sr=0.2,M=0.5,K=0.5

s=0,0.3,0.5,0.9,1.5

Figure3c. Effect of suction parameters on
Figure4. Effect of Dufour Df on
          concentration profiles

β=0.1,Pr=1,γ=2,λ=1,N=1,Nt=0.1,
Nb=0.8,Le=1,Sr=0.2,M=0.5,K=0.5

Df=0.0, 0.2, 0.4, 0.6,1.0
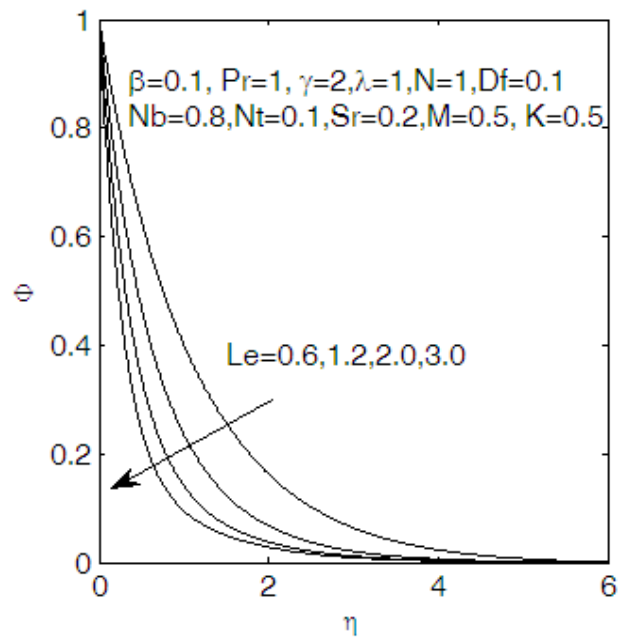
temperature profiles
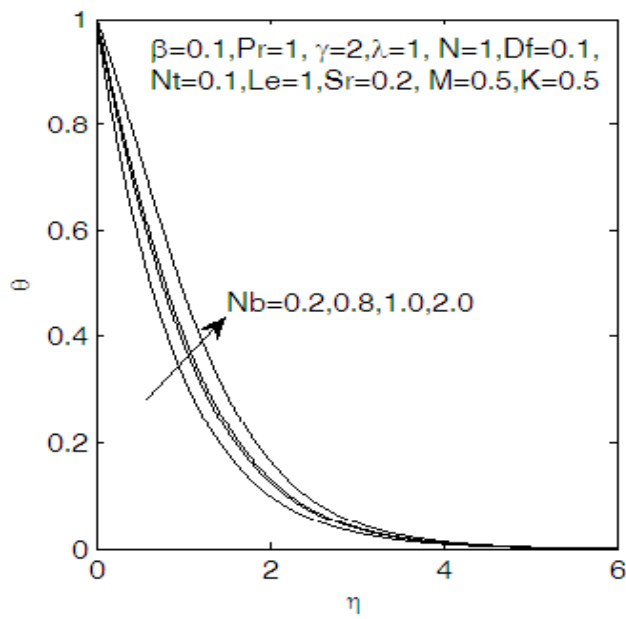
Figure5a. Effect of Brownian motion
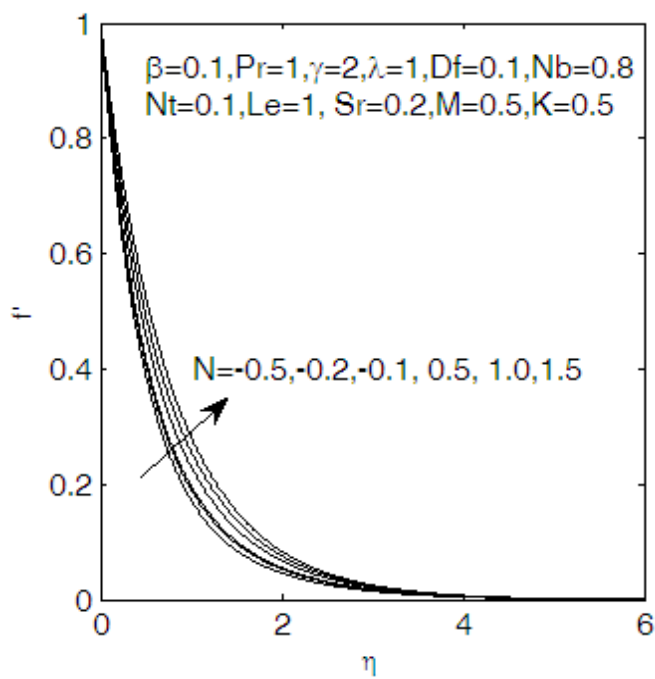parameter Nb on temperature profiles
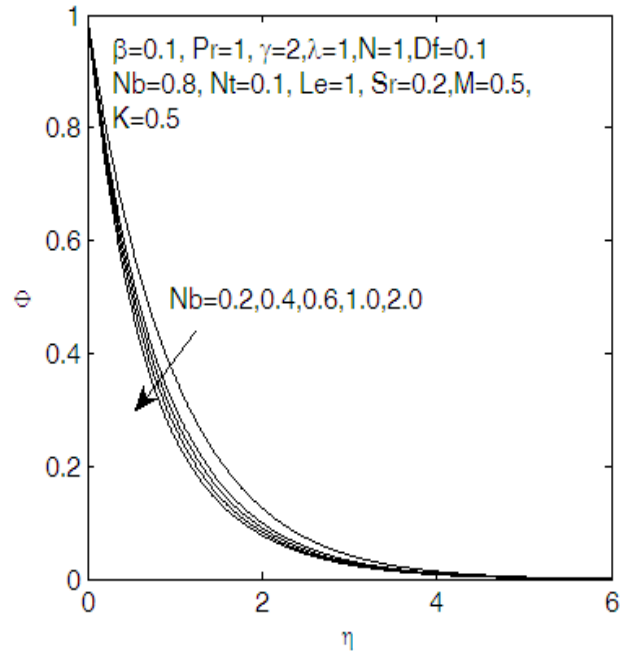
Figure5b. Effect of Brownian motion
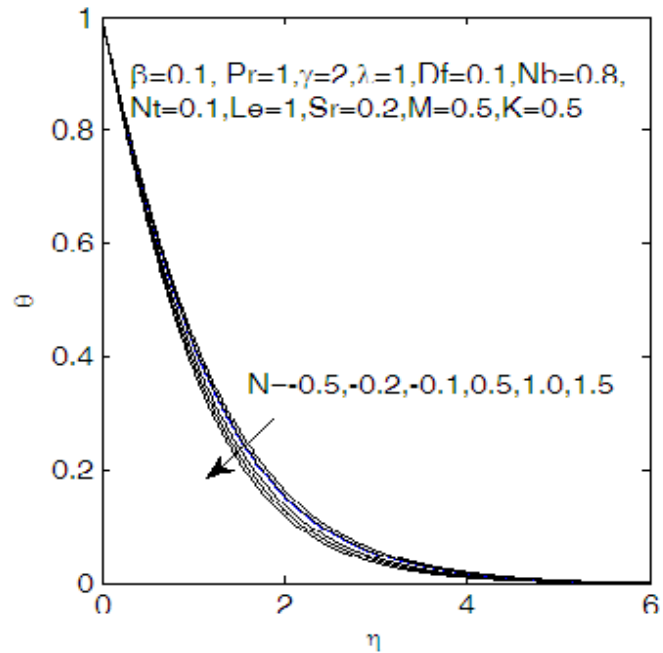parameter Nb on concentration profiles.
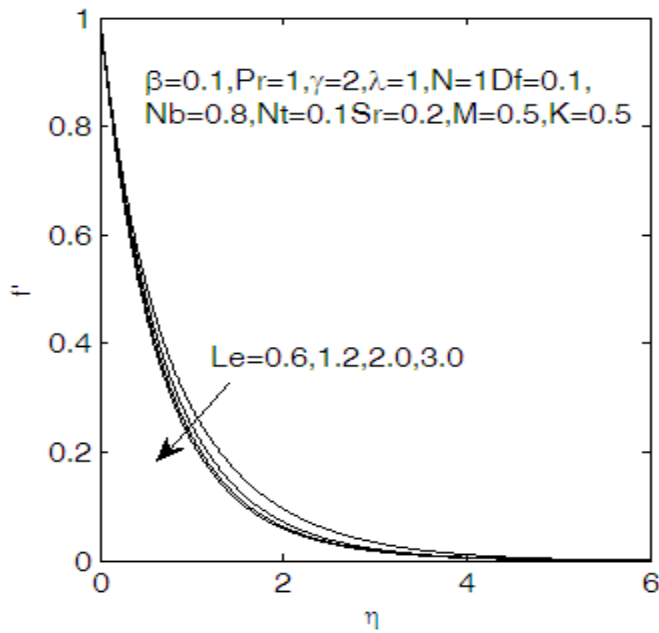
Figure6a. Effect of Lewis number Le on
velocity profiles.

Figure6b. Effect of Lewis number Le
on Concentration profiles.

Applications and Applied Mathematics: An International Journal (AAM), Vol. 15 [], Iss. 1, Art. 31

AAM: Intern. J., Vol. 15, Issue 1 (June 2020)   549

Figure7a. Effect of buoyancy parameter
N on velocity profiles

Figure7b. Effect of buoyancy N on
temperature profiles.